

Influence of InGaN waveguide on injection efficiency in III-nitride laser diodes

MATEUSZ HAJDEL*, GRZEGORZ MUZIÓŁ, KRZESIMIR NOWAKOWSKI-SZKUDLAREK, MARCIN SIEKACZ, PAWEŁ WOLNY, CZESŁAW SKIERBISZEWSKI

Institute of High Pressure Physics “Unipress”, PAS,
Sokołowska 29/37, 01-142 Warsaw, Poland

*Corresponding author: hajdel@unipress.waw.pl

The influence of using InGaN waveguides on blue laser diodes was theoretically studied using 1D drift diffusion model and 2D optical mode calculation. Despite of the known effect of increased confinement of an optical mode, especially for long wavelengths, an unexpected influence on the efficiency of carrier injection into the active region is discussed. It is found that InGaN-AlGaIn interface is crucial to achieving high injection efficiency. A numerical model is created, which describes the influence of InGaN waveguide and Mg doping of electron blocking layer on basic properties of laser diodes. It is found that an increase of injection efficiency allows to reduce the doping level in an electron blocking layer and take advantage of decreased optical losses.

Keywords: InGaN, laser diodes, waveguide, injection efficiency.

1. Introduction

The III-nitride laser diodes (LDs) are promising candidates to being reliable, cheap, and efficient light sources for variety of applications such as general lighting, laser projectors and data storage systems [1]. In the majority of violet InGaN LDs the GaN waveguides (WGs) are used [2]. However, in long wavelength devices, the optical mode is less confined with the active region [3–6]. The refractive index contrast between GaN waveguide and AlGaIn claddings drops, which causes the decrease of optical confinement factor Γ [5]. Theoretical and experimental studies have shown that replacing GaN with InGaN WGs can increase the confinement of the optical mode with the active region, especially for lasers emitting longer wavelengths (>450 nm) [7–9]. Additionally, InGaN WGs can be successfully used to ensure a good quality laser beam by preventing mode leakage to the substrate [10].

The main bottleneck which prevented the commercialization of III-nitride LDs was high optical losses caused in majority by Mg-doped layers [11–13]. This problem has

been solved by inserting an undoped layer between quantum wells and Mg-doped layers, which decreased the overlap of the optical field with these layers. Introducing the InGaN WGs also changes the confinement in Mg-doped layers and can reorder their contribution to overall optical losses α_i . Special attention should be given to the electron blocking layer (EBL) since it is the highest p-type doped layer placed right after the active region to prevent carrier overflow and ensure high carrier injection efficiency η_i into quantum wells. High Mg doping in EBL is necessary to ensure high η_i . Low α_i and high η_i are crucial to obtain high efficiency LD with low threshold current.

In this work we show via theoretical simulations that the InGaN WGs not only increase Γ and decrease losses originating from Mg doped layers but also increase η_i . This can be used to further improve the performance of III-nitride LDs by a decrease of the Mg-doping level in EBL and thus obtain a reduction of α_i .

2. Simulation framework

To study band diagrams and η_i values of III-nitride LDs, the 1D drift diffusion model simulation was performed using SiLENSe 5.4 software [14]. 2D optical waveguide calculations were performed by CAMFR module [15]. Based on the refractive index profile, the optical mode distribution was calculated and used to estimate confinement factors. A simple linear model correlating Mg concentration with light absorption was assumed. Based on our previous experimental study, a relation $\alpha_{\text{Mg}} = 112 \text{ cm}^2 \times \text{Mg concentration}$ (in units of 10^{19} cm^{-3}) was determined [16].

The considered structure is shown in Fig. 1 and consists of 700 nm $\text{Al}_{0.07}\text{Ga}_{0.93}\text{N}:\text{Si}$ bottom cladding and 100 nm $\text{GaN}:\text{Si}$ – both layers have a silicon doping level of

SiO ₂	100 nm Au	SiO ₂
	65 nm $\text{In}_{0.02}\text{Ga}_{0.98}\text{N}:\text{Mg}$	
	VI 600 nm $\text{Al}_{0.02}\text{Ga}_{0.98}\text{N}:\text{Mg}$	
V	100 nm $\text{GaN}:\text{Mg}$	
III	20 nm $\text{Al}_{0.13}\text{Ga}_{0.87}\text{N}:\text{Mg}$	
II	110 nm $\text{In}_{0.04}\text{Ga}_{0.96}\text{N}$	
I	25 nm $\text{In}_{0.17}\text{Ga}_{0.83}\text{N}$	
II	110 nm $\text{In}_{0.04}\text{Ga}_{0.96}\text{N}$	
IV	100 nm $\text{GaN}:\text{Si}$	
VII	700 nm $\text{Al}_{0.07}\text{Ga}_{0.93}\text{N}:\text{Si}$	
	50 nm $\text{GaN}:\text{Si}$	
	100 μm GaN substrate	
	100 nm Au	

Fig. 1. Schematic of the simulated structure.

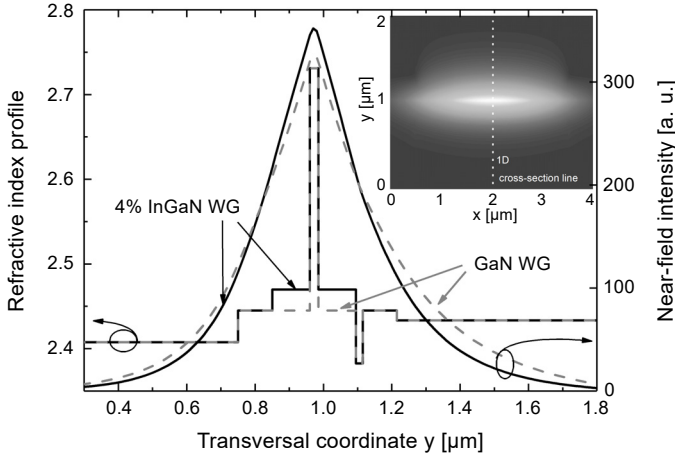


Fig. 2. Calculated 1D optical field distribution for LD with $\text{In}_{0.04}\text{Ga}_{0.96}\text{N}$ waveguide (solid line) and GaN waveguide (dashed line); insert presents 2D map of optical field for LD with $\text{In}_{0.04}\text{Ga}_{0.96}\text{N}$ waveguide.

$2 \times 10^{18} \text{ cm}^{-3}$. Waveguides are 110 nm $\text{In}_x\text{Ga}_{1-x}\text{N}$ undoped layers with x changed from 0 to 12%. On the top of the upper waveguide there is a 20 nm p-type $\text{Al}_{0.13}\text{Ga}_{0.87}\text{N}$ EBL. The Mg doping concentration is changed in EBL in the range from $2 \times 10^{18} \text{ cm}^{-3}$ to $6.5 \times 10^{19} \text{ cm}^{-3}$. Next the p-type region with the doping level of $1 \times 10^{18} \text{ cm}^{-3}$ consisting of 100 nm GaN and 600 nm $\text{Al}_{0.02}\text{Ga}_{0.98}\text{N}$ upper cladding is placed. This is capped with 65 nm $\text{In}_{0.02}\text{Ga}_{0.98}\text{N}$ contact layer. The active region of LD consists of a single 25 nm thick $\text{In}_{0.17}\text{Ga}_{0.83}\text{N}$ quantum well [17, 18]. An exemplary cross-section of the optical mode is presented in Fig. 2. In calculation, the 3 μm wide and 670 nm high mesa covered with SiO_2 on both sides is considered. Gold contacts are on the top of the mesa and on the bottom of the substrate.

3. Results and discussion

3.1. Influence of InGaN waveguide on mode overlap with Mg-doped layers

As was previously shown, replacing the GaN with InGaN waveguide in III-nitride LD increases the confinement of the optical mode with the active region, because of higher refractive index of InGaN [7, 9]. The increase of mode confinement with the active region also changes the confinement factors Γ in other layers, so the overall contribution of these layers to total α_i will change. This is extremely important for designing LD structure with low optical losses. The changes in confinement factors of quantum well (QW), WGs, EBL, and layers adjacent to the QW as a function of indium composition in WGs are shown in Fig. 3.

The obvious consequence of increasing indium content in waveguides is an increase of Γ with the active region (black solid line in Fig. 3), which should have a positive influence on device performance by decreasing threshold current density j_{th} . However, one has to remember that all confinement factors are influenced. The most important

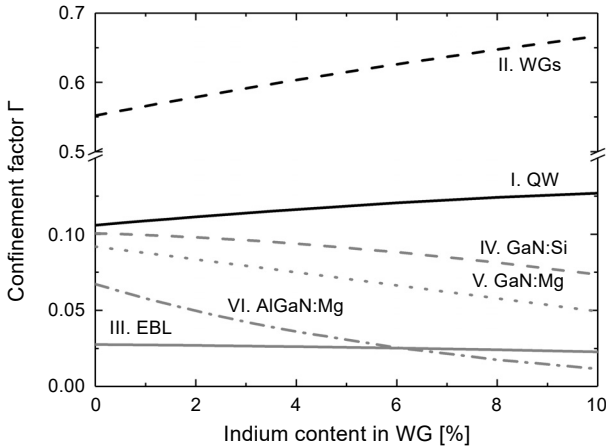


Fig. 3. Dependence of confinement factors of different layers on In content in waveguide.

are the waveguide itself and Mg-doped layers. The Γ of waveguide is equal to 0.552 and 0.667 for $x = 0.00$ and $x = 0.10$, respectively. Such a high overlap of the optical mode with WG can cause severe increase of α_i if absorption coefficient α_{InGaN} increases with In content. In principle, the Urbach tail in high In content InGaN might cause some absorption losses. However, at this point, there is still an open question due to the lack of experimental data. In the future it is necessary to perform separate experiments to estimate the influence of InGaN WG on α_i .

We found that, in the studied range of In content of InGaN WG (from GaN WG to 10% InGaN WG), the confinement factors of AlGaN and GaN p-type layers decreases from 0.067 to 0.012 and from 0.092 to 0.049, respectively. On the other hand, Γ_{EBL} (grey solid line) remains almost unchanged. It is worth noticing that Γ_{EBL} for high In content is almost half of $\Gamma_{\text{GaN:Mg}}$ and even larger than $\Gamma_{\text{AlGaN:Mg}}$. Usually EBL doping is an order of magnitude higher than other p-type layers. These two effects can lead to the domination of EBL over other p-type layers in terms of contribution to the total α_i , specially for high In content in waveguides.

3.2. Influence of InGaN waveguide on injection efficiency

We will determine now, the influence of In content in WG on electrical and carrier transport properties. Drift diffusion simulation was used to calculate the η_i and the results are shown in Fig. 4a. It is important to stress that the η_i depends on current density. For low current densities $j < 200 \text{ A/cm}^2$, the η_i is close to unity up to the 8% In in the waveguide composition. However, for higher current densities a decrease of η_i is observed. This drop is more significant for low In content in the waveguide. For In content higher than 8%, the η_i is lower than unity even at low current densities. This leads to the existence of optimum value of In content in WG somewhere around 8%. For a typical operating current densities $j = 3.5 \text{ kA/cm}^2$, injection the efficiency equals 0.65,

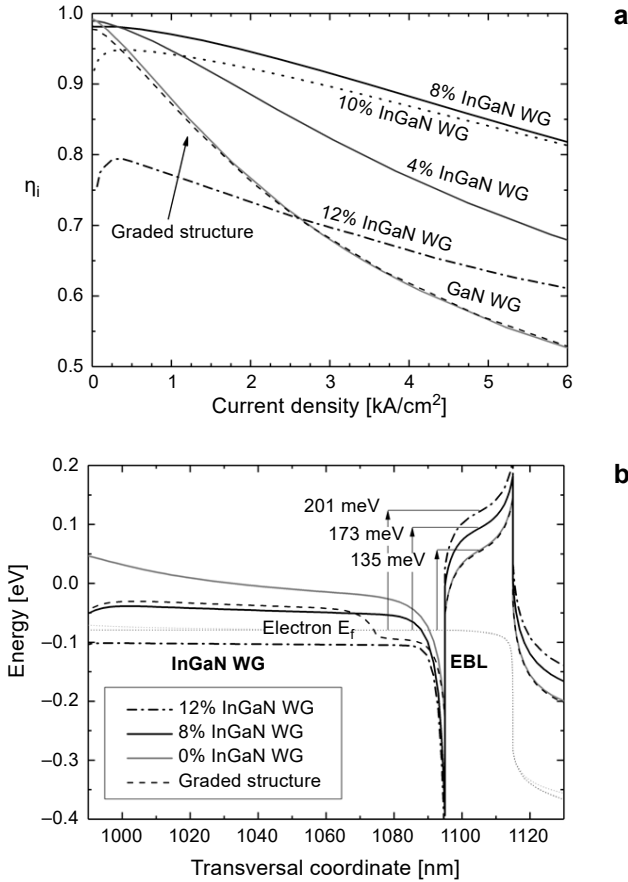


Fig. 4. Dependence of injection efficiency η_i calculated with drift diffusion model on current density (a). Part of conduction band profile for GaN, 8%, 12% and graded InGaN waveguide. Graded structure consists of 90 nm 8% InGaN and 20 nm pre-EBL grading regime from 8% InGaN to GaN. EBL doping level is constant Mg: $2 \times 10^{19} \text{ cm}^{-3}$ (b).

0.90 and 0.68 for GaN, 8% and 12% InGaN waveguides, respectively. Therefore, for constant doping level of EBL, the InGaN WGs, up to 8% In content, provide better carrier injection to active region. From this point of view, the use of InGaN WGs is beneficial for realizing efficient LD devices.

To explain the origin of the difference in η_i invoked by InGaN WG, the band diagrams are shown in Fig. 4b. The conduction bands were calculated for $j = 3.5 \text{ kA/cm}^2$. The energy barrier created by EBL is equal to 135, 173, and 201 meV for GaN, 8% and 12% InGaN WG, respectively. The increase of EBL barrier height is responsible for an initial increase of η_i . However, for In content higher than 8%, η_i starts to drop as can be seen in Fig. 4a. This is a result of additional carrier accumulation in the WG regime, which causes unwanted recombination. Interestingly, the whole positive im-

pect of InGaN WG on η_i arises only due to the difference in bandgaps at the WG and EBL interface. To show it, we have performed calculations on structure consisting of 8% InGaN WG but the composition is graded from 8% to 0% on the last 20 nm. The resulting structure has an interface between WG and EBL consisting of GaN and AlGaIn. Grading WG exhibits a similar Γ as 8% InGaN but η_i values are exactly the same as in the case of GaN WG. Therefore realization of the interface between AlGaIn and InGaN is crucial for ensuring high η_i . Similar effect of an increased carrier injection was observed if an InGaN layer is introduced between GaN WG and AlGaIn EBL [19]. Then, an InGaN-AlGaIn interface is formed.

As was mentioned previously, one of the drawbacks of using InGaN waveguides, despite technological issues in growing high indium content thick layers [20, 21], is higher carrier accumulation [19, 22]. MEHARI *et al.* [22] found that in semipolar InGaIn LDs, when a part of GaN waveguide is replaced by InGaIn layer, carriers accumulate in WG. The carrier concentration in the order of 10^{19} cm^{-3} was found to decrease η_i due to unwanted recombination of carriers. This problem can be solved by starting WG layer with InGaIn without the unintentionally doped GaN layer. In Fig. 5 the band profiles and carrier concentrations of previously described 8% InGaIn WG structure and structure with 20 nm GaN layer placed between QW and InGaIn WG are shown. When GaN layer is present, the carrier concentration in InGaIn WG equals $6 \times 10^{18} \text{ cm}^{-3}$. By using fully InGaIn waveguide, the carriers do not accumulate and concentration drops by an order of magnitude. The relative EBL barrier height is the same in these two structures.

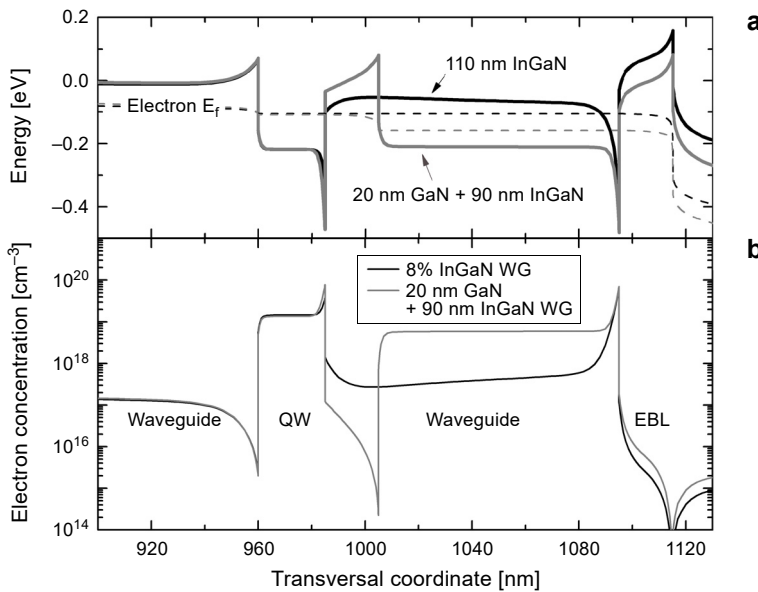


Fig. 5. Conduction band profile (a) and electron concentration (b) in waveguide layers for structures with full 8% InGaIn (black line) and with GaN layer between QW and WG (grey line) for $j = 3.5 \text{ kA/cm}^2$ based on drift diffusion simulations.

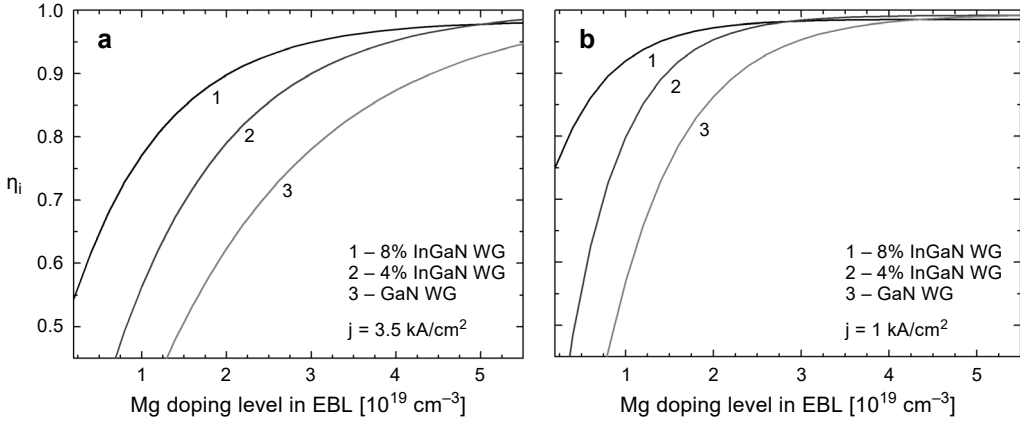


Fig. 6. Calculated injection efficiency as a function of EBL doping level for different InGaN waveguide compositions for current density 3.5 kA/cm² (a), and 1 kA/cm² (b).

Because of the influence of WG composition on the EBL height, the doping level of EBL has to be also discussed since doping itself strongly affects the barrier height [16]. As was discussed in Section 3.1, the EBL contribution to α_i for high In content WGs increases, so desirably the Mg level should be kept as low as possible. Figures 6a and 6b present the calculated dependence of η_i on Mg doping for current densities of 3.5 and 1 kA/cm², respectively. For $j = 3.5$ kA/cm² and high Mg doping ($\text{Mg} > 4 \times 10^{19}$ cm⁻³), the η_i is close to unity. For Mg doping $\text{Mg} = 2 \times 10^{19}$ cm⁻³, the η_i is still close to unity only for 8% InGaN WG. Therefore for lower InGaN compositions the η_i drops. As a result, one can achieve equal η_i for GaN WG and 4.3×10^{19} cm⁻³ Mg concentration and 8% InGaN and 2×10^{19} cm⁻³ Mg. To keep the η_i on acceptable level and take advantage of the decreased α_i , the high In content WGs has to be used. The η_i decrease rate is noticeably lower for high In, thus the Mg content can be more reduced in these structures. Even higher enhancement can be achieved if threshold current density could be lowered to 1 kA/cm². As can be seen in Fig. 6b, high η_i can be achieved even for Mg doping as low as 1×10^{19} cm⁻³. Importantly, decrease of j_{th} can be obtained by decreasing the Mg doping level. A lower Mg level can therefore help in achieving lower j_{th} if the η_i is kept at high values.

3.3. Modelling the operating parameters of LDs

For describing the influence of InGaN waveguides on the operation of real LD, the parameters such as threshold current density j_{th} and slope efficiency SE will be discussed. Both of them are related to η_i and α_i through [23]:

$$j_{\text{th}} = \frac{\alpha_i + \alpha_m}{\eta_i \Gamma_{\text{active}} \frac{dg}{dj}} + j_{\text{trans}} \quad (1)$$

$$SE = \eta_i \frac{\alpha_m}{\alpha_i + \alpha_m} \frac{h\nu}{q} \quad (2)$$

where g is the material gain, Γ_{active} is the confinement factor of active region, j_{trans} is the transparency current, α_m are mirror losses, ν is the frequency of emitted light, q is the elementary charge, and h is the Planck constant; α_i is the sum of losses originating from highly doped EBL α_{EBL} and additional losses from other layers α_0 . The Mg doped layers absorption coefficient α_{Mg} is assumed to increase linearly with Mg doping through the relation $\alpha_{\text{Mg}} = 112 \text{ cm}^2 \times \text{Mg concentration}$ (in units of 10^{19} cm^{-3}), which was found in our previous paper [16]. The α_{EBL} for Mg: $2 \times 10^{19} \text{ cm}^{-3}$ equals 5.4, 5.9, and 6.2 cm^{-1} , for 8%, 4% and 0% InGaIn WG, respectively. Internal losses that originate from all other layers expect to be EBL are assumed to be a product of absorption coefficients and calculated confinement factors. Due to the low doping in other layers, the α_0 is independent of WG composition and is equal to $\alpha_0 = (9.5 \pm 0.05) \text{ cm}^{-1}$. The model lacks a dependence of absorption in InGaIn WG on In composition.

Taking into consideration that η_i and Γ change with In content in WG, the theoretical j_{th} and SE values were calculated and presented in Figs. 7a and 7b. There is an interplay of η_i and α_{Mg} which causes a complicated dependence of j_{th} and SE on Mg doping level in EBL. In the low doping regime, the j_{th} is high and SE is low due to electron overflow and thus low η_i . As the doping level is increased, j_{th} and SE both improve up to a point, in which the increase in η_i is insignificant. Then an increase in j_{th} and decrease of SE can be observed due to increasing α_{Mg} .

General enhancement of LD operating parameters for high In composition is observed due to the increased Γ and η_i . The η_i decrease rate is slower for higher In contents thus the shift of the optimum Mg doping level towards lower doping concentration is observed. From this analysis the optimum doping points for different In compositions are extracted and presented in Fig. 8 with black circles. Consequently, optimum device

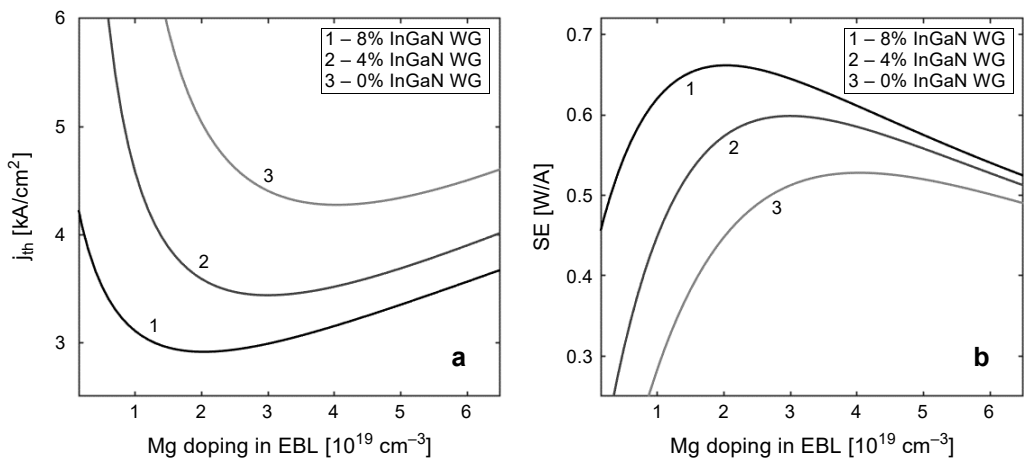


Fig. 7. Dependence of threshold current density (a) and slope efficiency (b) on EBL Mg doping level. LD operation wavelength is 450 nm. Resonator length is 1000 μm . Cleaved uncoated mirrors are assumed.

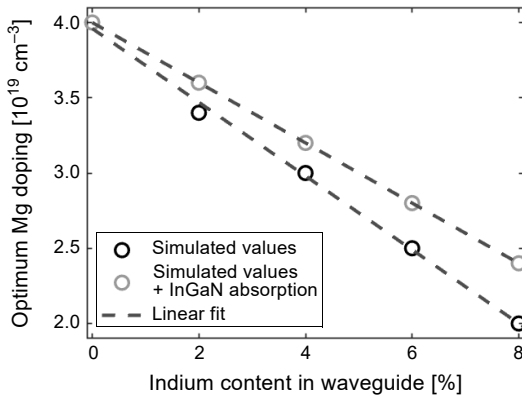


Fig. 8. Dependence of optimum EBL doping concentrations on In composition. The dependence for artificial absorption dependence on In content is also showed.

operation with GaN WGs requires higher Mg doping and therefore high optical losses are present. The high In structures have lower j_{th} which stands in agreement with previous experimental reports [8]. For devices with lower j_{th} , the observed difference between different WG designs is expected to be smaller since η_i decrease rate is smaller as can be seen in Fig. 6b. However, in devices with high In content WG, an additional source of optical losses may appear. To test the influence of absorption by InGaN WG on optimum Mg doping of EBL, we have assumed a linear increase of absorption coefficient with In content. In this model the absorption coefficient linearly increases with In content in such a way that 4% InGaN absorption coefficient increases by 10 cm^{-1} and 8% InGaN by 20 cm^{-1} . This is in our opinion an upper limit for undoped layer. The results are shown in Fig. 8 with grey circles. The linear decrease of optimum Mg doping in EBL on InGaN WGs composition is observed in both cases.

4. Conclusions

The influence of different compositions of InGaN waveguide on injection efficiency in III-nitride LDs was discussed. It is found that the increase of In composition in waveguides effectively increases the barrier of EBL and prevents the electron overshoot. We found that the application of InGaN waveguide can allow to reduce the Mg doping level in EBL and thus reduce the optical losses originating from this layer. The important role of InGaN-AlGaN interface in keeping high η_i was discussed. The high In content in InGaN WGs ensures also higher mode confinement in the active region and lower in layers causing high optical losses. Presented aspects lead to the increased performance of LD with InGaN WGs in comparison to the GaN ones.

Acknowledgements – This work has been partially supported by TEAMTECH POIR.04.04.00-00-210C/16-00 project of the Foundation for Polish Science co-financed by the European Union under the European Regional Development Fund and the National Centre for Research and Development grants LIDER/29/0185/L-7/15/NCBR/2016 and LIDER/35/0127/L-9/17/NCBR/2018.

References

- [1] WIERER J.J., TSAO J.Y., SIZOV D.S., *Comparison between blue lasers and light-emitting diodes for future solid-state lighting*, *Laser and Photonics Reviews* **7**(6), 2013 pp. 963–993, DOI: [10.1002/lpor.201300048](https://doi.org/10.1002/lpor.201300048).
- [2] KAWAGUCHI M., IMAFUJI O., NOZAKI S., HAGINO H., TAKIGAWA S., KATAYAMA T., TANAKA T., *Optical-loss suppressed InGaN laser diodes using undoped thick waveguide structure*, *Proceedings of SPIE* **9748**, 2016, article 974818, DOI: [10.1117/12.2212011](https://doi.org/10.1117/12.2212011).
- [3] ZHANG L.Q., JIANG D.S., ZHU J.J., ZHAO D.G., LIU Z.S., ZHANG S.M., YANG H., *Confinement factor and absorption loss of AlInGaN based laser diodes emitting from ultraviolet to green*, *Journal of Applied Physics* **105**(2), 2009, article 023104, DOI: [10.1063/1.3068182](https://doi.org/10.1063/1.3068182).
- [4] MUZIOL G., TURSKI H., SIEKACZ M., SAWICKA M., WOLNY P., PERLIN P., SKIERBISZEWSKI C., *Determination of gain in AlGaIn cladding free nitride laser diodes*, *Applied Physics Letters* **103**(6), 2013, article 061102, DOI: [10.1063/1.4817754](https://doi.org/10.1063/1.4817754).
- [5] LERMER T., SCHILLGALIES M., BREIDENASSEL A., QUEREN D., EICHLER C., AVRAMESCU A., MULLER J., SCHEIBENZUBER W., SCHWARZ U., LUTGEN S., STRAUSS U., *Waveguide design of green InGaN laser diodes*, *Physica Status Solidi (A)* **207**(6), 2010, pp. 1328–1331, DOI: [10.1002/pssa.200983410](https://doi.org/10.1002/pssa.200983410).
- [6] STRAUSS U., EICHLER C., RUMBOLZ C., LELL A., LUTGEN S., TAUTZ S., SCHILLGALIES M., BRÜNINGHOFF S., *Beam quality of blue InGaN laser for projection*, *Physica Status Solidi (C)* **5**(6), 2008, pp. 2077–2079, DOI: [10.1002/pssc.200778417](https://doi.org/10.1002/pssc.200778417).
- [7] HUANG C., LIN Y., TYAGI A., CHAKRABORTY A., OHTA H., SPECK J.S., DENBAARS S.P., NAKAMURA S., *Optical waveguide simulations for the optimization of InGaN-based green laser diodes*, *Journal of Applied Physics* **107**(2), 2010, article 023101, DOI: [10.1063/1.3275325](https://doi.org/10.1063/1.3275325).
- [8] MUZIOL G., TURSKI H., SIEKACZ M., WOLNY P., GRZANKA S., GRZANKA E., PERLIN P., SKIERBISZEWSKI C., *Enhancement of optical confinement factor by InGaN waveguide in blue laser diodes grown by plasma-assisted molecular beam epitaxy*, *Applied Physics Express* **8**(3), 2015, article 032103, DOI: [10.7567/APEX.8.032103](https://doi.org/10.7567/APEX.8.032103).
- [9] CHEN P., FENG M.X., JIANG D.S., ZHAO D.G., LIU Z.S., LI L., WU L.L., LE L.C., ZHU J.J., WANG H., ZHANG S.M., YANG H., *Improvement of characteristics of InGaN-based laser diodes with undoped InGaN upper waveguide layer*, *Journal of Applied Physics* **112**(11), 2012, article 113105, DOI: [10.1063/1.4768287](https://doi.org/10.1063/1.4768287).
- [10] MUZIOL G., TURSKI H., SIEKACZ M., GRZANKA S., PERLIN P., SKIERBISZEWSKI C., *Elimination of leakage of optical modes to GaN substrate in nitride laser diodes using a thick InGaN waveguide*, *Applied Physics Express* **9**(9), 2016, article 092103, DOI: [10.7567/APEX.9.092103](https://doi.org/10.7567/APEX.9.092103).
- [11] KIOUPAKIS E., RINKE P., SCHLEIFE A., BECHSTEDT F., VAN DE WALLE C.G., *Free-carrier absorption in nitrides from first principles*, *Physical Review B* **81**(24), 2010, article 241201(R), DOI: [10.1103/PhysRevB.81.241201](https://doi.org/10.1103/PhysRevB.81.241201).
- [12] UCHIDA S., TAKEYA M., IKEDA S., MIZUNO T., FUJIMOTO T., MATSUMOTO O., GOTO S., TOIYO T., IKEDA M., *Recent progress in high-power blue-violet lasers*, *IEEE Journal of Selected Topics in Quantum Electronics* **9**(5), 2003, pp. 1252–1259, DOI: [10.1109/JSTQE.2003.820910](https://doi.org/10.1109/JSTQE.2003.820910).
- [13] KURAMOTO M., SASAOKA C., FUTAGAWA N., NIDO M., YAMAGUCHI A.A., *Reduction of internal loss and threshold current in a laser diode with a ridge by selective re-growth (RiS-LD)*, *Physica Status Solidi (A)* **192**(2), 2002, pp. 329–334, DOI: [10.1002/1521-396X\(200208\)192:2%3C329::AID-PSA3329%3E3.0.CO;2-A](https://doi.org/10.1002/1521-396X(200208)192:2%3C329::AID-PSA3329%3E3.0.CO;2-A).
- [14] SiLENSe 5.4 package, <http://str-soft.com/products/SiLENSe/> (accessed October 12, 2019).
- [15] CAMFR (CAvity Modelling FRamework), <http://camfr.sourceforge.net> (accessed October 12, 2019).
- [16] HAJDEL M., MUZIOL G., NOWAKOWSKI-SZKUDLAREK K., SIEKACZ M., FEDUNIEWICZ-ŻMUDA A., WOLNY P., SKIERBISZEWSKI C., *Influence of electron blocking layer on properties of InGaN-based laser diodes grown by plasma-assisted molecular beam epitaxy*, *Acta Physica Polonica A* **136**(4), 2019, pp. 593–597, DOI: [10.12693/APhysPolA.136.593](https://doi.org/10.12693/APhysPolA.136.593).

- [17] MUZIOL G., HAJDEL M., SIEKACZ M., SZKUDLAREK K., STANCZYK S., TURSKI H., SKIERBISZEWSKI C., *Optical properties of III-nitride laser diodes with wide InGaN quantum wells*, Applied Physics Express **12**(7), 2019, article 072003, DOI: [10.7567/1882-0786/ab250e](https://doi.org/10.7567/1882-0786/ab250e).
- [18] MUZIOL G., TURSKI H., SIEKACZ M., SZKUDLAREK K., JANICKI L., BARANOWSKI M., ZOLUD S., KUDRAWIEC R., SUSKI T., SKIERBISZEWSKI C., *Beyond quantum efficiency limitations originating from the piezoelectric polarization in light-emitting devices*, ACS Photonics **6**(8), 2019, pp. 1963–1971, DOI: [10.1021/acsp Photonics.9b00327](https://doi.org/10.1021/acsp Photonics.9b00327).
- [19] LE L.C., ZHAO D.G., JIANG D.S., CHEN P., LIU Z.S., YANG J., HE X.G., LI X.J., LIU J.P., ZHU J.J., ZHANG S.M., YANG H., *Suppression of electron leakage by inserting a thin undoped InGaN layer prior to electron blocking layer in InGaN-based blue-violet laser diodes*, Optics Express **22**(10), 2014, pp. 11392–11398, DOI: [10.1364/OE.22.011392](https://doi.org/10.1364/OE.22.011392).
- [20] HOLEC D., COSTA P.M.F.J., KAPPERS M.J., HUMPHREYS C.J., *Critical thickness calculations for InGaN/GaN*, Journal of Crystal Growth **303**(1), 2007, pp. 314–317, DOI: [10.1016/j.jcrysgro.2006.12.054](https://doi.org/10.1016/j.jcrysgro.2006.12.054).
- [21] LEYER M., STELLMACH J., MEISSNER CH., PRISTOVSEK M., KNEISSL M., *The critical thickness of InGaN on (0 0 0 1)GaN*, Journal of Crystal Growth **310**(23), 2008, pp. 4913–4915, DOI: [10.1016/j.jcrysgro.2008.08.021](https://doi.org/10.1016/j.jcrysgro.2008.08.021).
- [22] MEHARI S., COHEN D.A., BECERRA D.L., NAKAMURA S., DENBAARS S.P., *Semipolar InGaN blue laser diodes with a low optical loss and a high material gain obtained by suppression of carrier accumulation in the p-waveguide region*, Japanese Journal of Applied Physics **58**(2), 2019, article 020902, DOI: [10.7567/1347-4065/aaf4b4](https://doi.org/10.7567/1347-4065/aaf4b4).
- [23] COLDREN L.A., CORZINE S.W., MAŠANOVIĆ M.L., *Diode Lasers and Photonic Integrated Circuits*, Second Edition, Wiley, 2012, pp. 45–246, DOI: [10.1002/9781118148167](https://doi.org/10.1002/9781118148167).

Received October 16, 2019
in revised form January 8, 2020